LEVEL II

B.S. 12

THE GEORGE WASHINGTON UNIVERSITY

AD A087017

STUDENTS FACULTY STUDY R ESEARCH DEVELOPMENT FUT URE CAREER CREATIVITY CC MMUNITY LEADERSHIP TECH NOLOGY FRONTIE ESIGN ENGINEERING APP ENC GEORGE WASHIN NIV

SCHOOL OF ENGINEERING AND APPLIED SCIENCE

(12)

(6)

NONLINEAR CREEP BUCKLING ANALYSIS OF INITIALLY IMPERFECT SHALLOW SPHERICAL SHELLS

(10) Robert Kao

Sponsored by

Office of Naval Research

Arlington, Virginia 22217

Contract Number

(15) NAVY N00014-75-C-0946

(12) 50

(11) July 1980

School of Engineering and Applied Science

The George Washington University

Washington, D.C. 20052

NONLINEAR CREEP BUCKLING ANALYSIS OF INITIALLY IMPERFECT SHALLOW SPHERICAL SHELLS[1]

by

Robert Kao

July 1980

Department of Civil, Mechanical, and Environmental Engineering
The George Washington University
Washington, D. C. 20052

[1] The research reported on here was supported by the Office of Naval Research, Contract Number NAVY 00014-75-C-0946

ABSTRACT

Creep deformations and creep buckling times are obtained for axisymmetric shallow spherical shells with and without initial imperfections. For nonlinear creeps, both strain-hardening and time-hardening rules are employed in the analysis; results indicate that strain-hardening yields better estimates of shell life than time-hardening. Results also show that the initial imperfection plays an important role in shortening shell creep buckling times. When compared with the experimental data of test specimens which possess very small departures from sphericity, it is observed that, in order to have a satisfactory prediction on both creep buckling times and creep deformations, in addition to fully taking into account the presence of initial imperfections, the analysis should adopt a mathematical creep model which includes not only the primary and the secondary creep but also the tertiary creep.

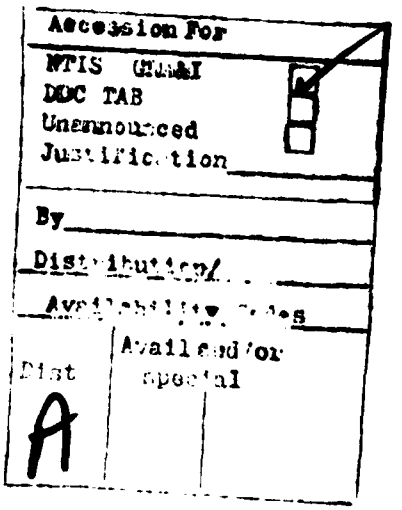

INTRODUCTION

It is well known that thin-walled structures, whose material deforms in consequence of creep, collapse if applied loads of constant magnitude act upon them for a sufficient time [1]. For uniformly loaded spherical shells, it is found that the length of the collapse time depends on the magnitude of applied pressure [2]. The collapse time, as may also be called the creep buckling time or the structure life, is referred to the passage of time between load application and structure failure. The calculation of collapse times along with creep deformations for axisymmetric shallow spherical shells is of major interest in this paper.

A key element involved in the creep buckling analysis is the selection of constitutive equations to describe the creep behavior of the material [3-6]; an appropriate selection should provide a good approximation to the test data. If the equations selected only represent the secondary creep, a linear relationship between the creep strain and the time function evolves and the solution procedure to deal with this situation is very straightforward. On the other hand, if the equations represent either the primary or tertiary creep, a nonlinear relationship results. Two of widely adopted approaches to handle this rather complicated situation are time-hardening and strain-hardening rules [5,7]. In general, predictions based on these two

approaches are quite different, and a choice between them should depend on the comparison of their predictions with experimental data.

Another key element is initial imperfections which, on many occasions, are directly resulted from the unavoidable inaccuracy of manufacturing process. It has been shown that initial imperfections have a great impact on reducing buckling pressures of spherical shells in both static and dynamic responses [8-10]. As to their influence in the creep buckling analysis, there has been an indication that the collapse time of cylindrical shells is very much affected by the imperfection magnitude [11,12].

In an earlier creep buckling analysis of shallow spherical shells [2], a huge discrepancy was found between theoretical predictions and experimental results on creep deformations and collapse times. The shell specimens used in experiments involved small departures from sphericity. But the theoretical study on the same specimens was performed by assuming the shells had no imperfections. Therefore, it may be quite reasonably to assume that initial imperfections, among other factors, are at least in part responsible for the aforementioned discrepancy.

The objective of this paper is to utilize the large deformation creep buckling procedure to obtain creep deformations and creep buckling times for simply supported shallow spherical shells subjected to uniform external

pressure. Solutions to be obtained include those of spherical caps with and without initial imperfections. A comparison of these solutions with experimental data [2] is intended to show the degree of sensitivity of the shell collapse time to initial imperfections. The comparison is also aimed at a close examination on the reliability of constitutive equations of creep adopted, from which a suggestion may be made on a more suitable choice of these equations to improve the theoretical predictions. As may be useful in practical designs, a plot of buckling pressure vs collapse time is presented which will demonstrate how the shell life expectancy is affected by the magnitude of applied pressure.

PROBLEM FORMULATION

The geometry of a spherical cap is shown in Fig. 1a, in which H is the central height and R the shell radius; a is the base radius; W(r) and U(r) are the displacement components along normal and tangential directions, respectively, and $W_i(r)$ is the initial imperfection; q is the applied uniform pressure. The undeformed shape of the perfect shell can be adequately described by

$$Z = H\,[1 - (r/a)^2] \tag{1a}$$

and the radius of curvature of the shell is approximated by

$$R = a^2/2H \tag{1b}$$

where r is the radial coordinate.

Figure 1b shows the membrane forces N_r and N_θ, the transverse shear Q_r and the moments M_r and M_θ. Equilibrium of moments requires

$$(rM_r)' - M_\theta - rQ_r = 0 \tag{2}$$

And equilibrium of stress resultants along radial and normal directions provides

$$(rN_r)' - N_\theta = 0 \tag{3}$$

$$[rN_r(W_f\text{-}Z)' + rQ_r]' + rq = 0 \tag{4}$$

where $(\ )' = \partial(\ )/\partial r$ and $W_f = W + W_i$. Note that the geometric nonlinearity has been introduced in Eq. (4) by considering the influence of W_f.

Elimination of Q_r in Eqs. (2) and (4) yields

$$M_r'' + \frac{2}{r} M_r' - \frac{1}{r} M_\theta' + N_r(W_f'' + \frac{1}{R}) + N_\theta(\frac{W_f'}{r} + \frac{1}{R}) + q = 0 \quad (5)$$

Eqs. (3) and (5) are the basic equations for the analysis of axisymmetric spherical caps.

Stress-Strain and Strain-Displacement Relations

For a shell undergoing the creep deformation after the existing load acts upon it for a certain period of time, the strain in a point within the thickness at a given time can be expressed by

$$\{e\} = \{e^e\} + \{e^c\} \quad (6)$$

where $\{e\}$, $\{e^e\}$ and $\{e^c\}$ are the total, elastic and creep strain vectors, respectively.

Furthermore, the total strain can be considered as the sum of the membrane and bending components:

$$\{e\} = \{\varepsilon\} + z\{\kappa\} \quad (7)$$

where z is the vertical coordinate through the shell thickness (Fig. 1b). The membrane and bending strains are related to displacements by

$$\begin{aligned} \varepsilon_r &= U' - \frac{W}{R} + \frac{1}{2}(W')^2 + W'W_i' \\ \varepsilon_\theta &= \frac{U}{r} - \frac{W}{R} \\ \kappa_r &= -W'' \\ \kappa_\theta &= -\frac{W'}{r} \end{aligned} \quad (8)$$

Note that the elastic components of strains are the only strains which can be related to stresses by Hook's law:

$$\{\sigma\} = [E]\ (\{e\} - \{e^c\}) \tag{9}$$

where [E], the elastic strain to stress transformation matrix, is given as

$$[E] = \frac{E}{1-\nu^2}\begin{bmatrix} 1 & \nu \\ \nu & 1 \end{bmatrix} \tag{10}$$

in which E is Young's modulus and ν is Poisson's ratio.

Membrane stress resultants and bending moments are obtained by

$$\{N\} = \int_{-h/2}^{h/2} \{\sigma\}\, dz \tag{11}$$

$$\{M\} = \int_{-h/2}^{h/2} \{\sigma\}\, z dz \tag{12}$$

Substituting Eqs. (6-9) into Eqs. (11) and (12), we obtain the membrane forces

$$\begin{Bmatrix} N_r \\ N_\theta \end{Bmatrix} = \frac{Eh}{1-\nu^2}\begin{bmatrix} 1 & \nu \\ \nu & 1 \end{bmatrix}\begin{Bmatrix} \varepsilon_r \\ \varepsilon_\theta \end{Bmatrix} - \begin{Bmatrix} N_r^c \\ N_\theta^c \end{Bmatrix} \tag{13}$$

where the effective creep membrane forces are

$$\begin{Bmatrix} N_r^c \\ N_\theta^c \end{Bmatrix} = [E] \int_{-h/2}^{h/2} \begin{Bmatrix} e_r^c \\ e_\theta^c \end{Bmatrix} dz \tag{14}$$

and the moments

$$\begin{Bmatrix} M_r \\ M_\theta \end{Bmatrix} = D \begin{bmatrix} 1 & \nu \\ \nu & 1 \end{bmatrix} \begin{Bmatrix} \kappa_r \\ \kappa_\theta \end{Bmatrix} - \begin{Bmatrix} M_r^c \\ M_\theta^c \end{Bmatrix} \tag{15}$$

where $D = Eh^3/12\ (1-\nu^2)$, and effective creep moments are

$$\begin{Bmatrix} M_r^c \\ M_\theta^c \end{Bmatrix} = [E] \int_{-h/2}^{h/2} \begin{Bmatrix} e_r^c \\ e_\theta^c \end{Bmatrix} z\,dz \tag{16}$$

Governing Equations

In terms of displacements, the governing equation involving the major displacement U is obtained by substituting Eqs. (13) and (14) into Eq. (3):

$$U'' + \frac{U'}{r} - \frac{U}{r^2} + G\ (W) = \frac{1-\nu^2}{Eh}\ q_1^c \tag{17}$$

where

$$\begin{aligned} G\ (W) &= F_r'(W) + \nu F_\theta'(W) + \frac{1-\nu}{r}(F_r - F_\theta) \\ F_r\ (W) &= -\ W/R + (W')^2/2 + W'W_i' \\ F_\theta\ (W) &= -\ W/R \\ F_r'\ (W) &= -\ W'/R + W'W'' + W'W_i'' + W''W_i' \\ F_\theta'\ (W) &= -\ W'/R \end{aligned} \tag{18}$$

and q_1^c, an effective creep load, is expressed in terms of effective creep membrane forces by

$$q_1^c = (N_r^c)' + N_r^c/r - N_\theta^c/r \tag{19}$$

The governing equation involving the major displacement W is also obtained by substituting Eqs. (13-16) into Eq. (5):

$$D\nabla^4 W - \frac{Eh}{1-\nu^2}(\varepsilon_r+\nu\varepsilon_\theta)(W_f''+1/R) - \frac{Eh}{1-\nu^2}(\varepsilon_\theta+\nu\varepsilon_r)(W_f'/r + 1/R)$$

$$= q - q_2^c - q_3^c \tag{20}$$

where $\nabla^4 = \nabla^2(\nabla^2)$ and $\nabla^2( ) = ( )'' + ( )'/r$; the membrane strains ε_r, ε_θ are defined in Eqs. (8), effective creep loads q_2^c and q_3^c are given as

$$q_2^c = N_r^c\ (W_f''+1/R) + N_\theta^c\ (W_f'/r+1/R) \tag{21}$$

$$q_3^c = (M_r^c)'' + 2\ (M_r^c)'/r - (M_\theta^c)'/r \tag{22}$$

Eqs. (17) and (20) are two fundamental governing equations in terms of displacements for the present analysis.

Boundary Conditions

At shell apex, the nature of axisymmetry requires that

$$W'(0) = 0 \tag{23}$$

$$U(0) = 0 \tag{24}$$

Along the outer edge ($r=a$), if the cap is clamped:

$$U(a) = W(a) = W'(a) = 0 \tag{25}$$

On the other hand, if the cap is simply supported, it re-

quires that

$$U\ (a) = W\ (a) = 0 \tag{26a}$$

and that $M_r\ (a)$ in Eq. (15) to be zero, i.e.,

$$D(\frac{d^2W}{dr^2} + \frac{\nu}{r}\frac{dW}{dr}) = -\ M_r^c\ (a), \quad r = a \tag{26b}$$

where M_r^c is defined in Eq. (16).

Nondimensional Forms

For convenience, the following nondimensional quantities are introduced

$$\begin{aligned} x &= r/a & m^4 &= 12(1-\nu^2) \\ \lambda^2 &= m^2a^2/Rh & q_{cr} &= 4Eh^2/R^2m^2 \\ (\ )' &= \partial(\ )/\partial x & p &= q/q_{cr} \\ u &= aU/h^2 & w_i &= W_i/h \\ w &= W/h \end{aligned} \tag{27}$$

where q_{cr} is the classical buckling pressure of a complete spherical shell of the same radius of curvature and thickness. With the adoption of Eqs. (27), the nondimensional forms of Eqs. (17) and (20) become

$$u'' + \frac{u'}{x} - \frac{u}{x^2} + g(w) = \frac{(1-\nu^2)\ a^3}{Eh^3}\ q_1^c \tag{28}$$

and

$$\nabla^4 w - 12(\bar{\varepsilon}_r+\nu\bar{\varepsilon}_\theta)\left(w_f'' + \frac{\lambda^2}{m^2}\right) - 12(\bar{\varepsilon}_\theta+\nu\bar{\varepsilon}_r)\left(\frac{w_f'}{x} + \frac{\lambda^2}{m^2}\right)$$

$$= 4\,\frac{\lambda^4}{m^2}\,p - \frac{m^4 a^4}{Eh^4}(q_2^c+q_3^c) \qquad (29)$$

where g (w) and f (w) terms are nondimensional counterparts of similar terms in Eq. (18):

$$g\,(w) = f_r'(w) + \nu f_\theta'(w) + (1-\nu)[f_r(w) - f_\theta(w)]/x$$

$$f_r(w) = -\frac{\lambda^2}{m^2}\,w + \frac{1}{2}(w')^2 + w'w_i'$$

$$f_\theta(w) = -\frac{\lambda^2}{m^2}\,w \qquad (30)$$

$$f_r'(w) = -\frac{\lambda^2}{m^2}\,w' + w'w'' + w'w_i'' + w''w_i'$$

$$f_\theta'(w) = -\frac{\lambda^2}{m^2}\,w'$$

and $\bar{\varepsilon}_\theta$, $\bar{\varepsilon}_\theta$ are nondimensional quantities of membrane strains ε_r and ε_θ in Eq. (8)

$$\bar{\varepsilon}_r = u' - \frac{\lambda^2}{m^2}\,w + \frac{1}{2}(w')^2 + w'w_i''$$

$$\bar{\varepsilon}_\theta = \frac{u}{x} - \frac{\lambda^2}{m^2}\,w \qquad (31)$$

CREEP THEORY

A typical uniaxial creep strain vs time curve under constant stress for most material used in engineering struc-

tures is shown in Fig. 2. The first part of this curve is known as the primary creep, a large portion of which is recoverable after unloading. The second part is identified as the steady creep, which possesses a linear creep strain-time relationship. The last part of this curve is called the tertiary creep where the strain rate increases until fracture occurs. In the present study, we only consider the primary and secondary creep.

In general, the uniaxial creep strain e^c in all stages of creep can be expressed by

$$e^c = Kf(\sigma)\, g(t) \tag{32}$$

where σ, t are stress and time function, respectively; K is a material constant.

When Eq. (32) is applied to the case of steady creep, we have $g(t) = t$ and

$$\dot{e}^c = de^c/dt = Kf(\sigma) \tag{33}$$

A very widely adopted empirical formula for Eq. (33) is the Norton equation:

$$\dot{e}^c = K\sigma^n \tag{34a}$$

or

$$\Delta e^c = K\sigma^n\, \Delta t \tag{34b}$$

where n is also a material constant.

The creep rate and the creep strain increment for the general expression, Eq. (32), are given in Eqs. (35a) and

(35b), respectively:

$$\dot{e}^c = Kf(\sigma)\ \dot{g}(t) \tag{35a}$$

$$\Delta e^c = Kf(\sigma)\ \dot{g}(t)\ \Delta t \tag{35b}$$

Equation (35b) represents the creep strain increment for the nonlinear creep such as the primary and tertiary creep.

A useful distinction among three different stages of creep (Fig. 2) may be obtained from the expression $\ddot{e}^c = d^2e^c/dt^2$ that the primary, steady and tertiary creeps are associated with $\ddot{e}^c < 0$, $\ddot{e}^c = 0$ and $\ddot{e}^c > 0$, respectively. In this study, the incremental procedure is employed to obtain solutions for creep problems, and hence, creep strains in their incremental forms such as Eqs. (34b) and (35b) are of primary importance.

When σ remains constant, the computation of Δe^c is very straightforward (Eq. (34b) or (35b)). However, if the computation is under the condition of varying stresses, the smooth stress-time curve is often approximated by horizontal and vertical segments as shown in Fig. 3a [13]. Within each segment, σ is assumed to be constant so that Eq. (34b) or (35b) can be applied.

For the nonlinear creep, two approaches are available to calculate Δe^c from Eq. (35b), namely, time-hardening and strain-hardening. Graphical representations of these two approaches are sketched in Fig. 3b and 3c for the strain-hardening and time-hardening theories, respectively. In

each figure, a number of constant stress e^c-t curves associated with various stress levels, and a varying stress e^c-t curve are shown.

First, let's discuss how to calculate Δe^c from the strain-hardening rule. At a generic point f' on the varying stress e^c-t curve of Fig. 3b, we have creep strain e^c_{k-1} at stress level σ_{k-1} and at time t_{k-1}. The value of t^*_{k-1} associated with point g on e^c-t curve for constant stress σ_k is computed by the following equation:

$$e^c_{k-1} = Kf(\sigma_k)\ g(t^*_{k-1}) \tag{36}$$

If the stress level changes from σ_{k-1} to σ_k, Δe^c for the next time increment Δt can be estimated approximately by

$$\Delta e^c = Kf(\sigma_k)\ \dot{g}(t^*_{k-1})\ \Delta t \tag{37a}$$

or be calculated exactly by

$$\Delta e^c = Kf(\sigma_k)\ g(t^*_{k-1}+\Delta t) - e^c_{k-1} \tag{37b}$$

If the computation is based on the time-hardening theory, Δe^c in Fig. 3c can be estimated approximately by

$$\Delta e^c = Kf(\sigma_k)\ \dot{g}(t_{k-1})\ \Delta t \tag{38a}$$

or be calculated exactly by

$$\Delta e^c = Kf(\sigma_k)\ g(t_{k-1}+\Delta t) - Kf(\sigma_k)\ g(t_{k-1}) \tag{38b}$$

The varying stress e^c-t curves shown in Fig. 3b and 3c, in fact, are obtained from the exact calculation formulas.

Since the slope of constant stress creep curves almost always decreases with time, except in the tertiary creep, a comparison between these two varying stress e^c-t curves in Fig. 3b and 3c indicates that strain-hardening predicts a higher creep strain than time-hardening.

In case of the steady creep, since the relationship between e^c and t is linear that these two approaches will yield the same result, the calculation of Δe^c should be very straightforward and the value so obtained is exact.

We shall generalize the calculation of creep strain increment from the uniaxial stress situation to the multiaxial state of stress. By adopting the same normality rule used in the formulation of plasticity theory as has been described in great details in Refs. [14,15,16,17], the creep strain in a multiaxial state of stress takes the form of

$$\Delta e^c_{ij} = \frac{\partial \sigma^*}{\partial \sigma_{ij}} \Delta e^c \tag{39}$$

where σ^*, the effective stress, is defined as

$$\sigma^* = \sqrt{\frac{3}{2} \sigma'_{ij} \sigma'_{ij}} \tag{40}$$

in which σ'_{ij}; the deviatoric stress, is given by

$$\sigma'_{ij} = \sigma_{ij} - \delta_{ij} \sigma \tag{41}$$

where δ_{ij} is Kronecker delta and σ is the hydrostatic stress.

After creep strain increments have been obtained, the current creep strains can easily be updated for the uniaxial

state of stress as

$$e_k^c = e_{k-1}^c + \Delta e^c \tag{42}$$

or for the multiaxial state of stress as

$$(e_{ij}^c)_k = (e_{ij}^c)_{k-1} + \Delta e_{ij}^c \tag{43}$$

COMPARISON WITH OTHER SOUTIONS

To test the validity and accuracy of creep theory adopted in this paper, two circular plate example problems are solved, solutions of which are compared with existing results. The first example is the bending of a simply supported circular plate under a constant uniform pressure (see Fig. 4). For simplicity, the analysis is restricted to the time during which the deflections are small so that the linear strain-displacement relations can apply. Elastic material is assumed with E(Young's modulus) = 7.4×10^6 psi and ν (Poisson's ratio) = 0.3. The plate geometry is outlined in the figure: R = 50 in. and h = 1 in.

Creep response is assumed in a state of steady creep, Eq. (34), with K = 1.491×10^{-15}/psi^3-hr and n = 3. These values correspond approximately to characteristics of 2024-T3 aluminum alloy at a temperature of 600°F. In the numerical solution process, a total of 10 evenly spaced nodal points along the meridian surface and 9 points across the plate thickness are chosen; a time increment of 50 hr. is also selected.

Results showing the time history of the maximum deflection for three load levels are displayed in Fig. 4. Also shown in the Figure are those of Ref. [18] in which a variational theorem for creep was formulated that was an extension of a variational theorem developed by Reissner. Despite the difference in the solution method employed, comparison between these two sets of results is quite favorable which tends to suggest the validity of the creep theory outlined in this paper.

The second example problem is also a simply supported circular plate but with the material of 75ST aluminum alloy at 600°F. and subjected to a uniformly distributed load of 36 psi (Fig. 5). The diameter of the plate is 10 in. and the thickness h is 0.5 in. Young's modulus of elasticity E for this material at 600°F. is 5.2×10^6 psi. Poisson's ratio is 0.3 for elastic strain and 0.5 for creep strain. The uniaxial creep strain-stress-time relation is nonlinear and for constant stress may be represented by

$$e^c = Ke^{A\sigma} t^B \tag{44}$$

where e^c and σ are the uniaxial creep strain and stress, respectively; the values of constant are $K = 2.64 \times 10^{-7}$, $A = 1.92 \times 10^{-3}$, t is in hr, $B = 0.66$.

The strain-hardening rule is selected to calculate the creep strain for different stress level; a time increment of 0.2 hr is used in the numerical computation. Results of deflection curves at $t = 0$, 1 hr are shown in Fig. 5. Also

shown in this figure are those obtained in Ref. [3] which employed a rather complicated solution scheme to solve governing equations with a time increment of 1 hr. The comparison between these two sets of results is quite good, and a better agreement between them may be expected should a smaller time increment be used in Ref. [3].

NONLINEAR CREEP BUCKLING OF AXISYMMETRIC SPHERICAL CAPS

Shell Model and Its Material Properties

A spherical cap model experimented in Ref. [2] is selected for the present analysis. The cap, under uniform external pressure and with simply supported boundary condition, possesses the following geometrical dimensions (Fig. 1): h (thickness) = 0.125 in., a (base radius) = 2.8387 in., R (shell radius) = 13.31 in., λ (geometric parameter) = 4.

The shell is made of Type 6/6 Nylon, whose creep property is assumed to obey a nonlinear uniaxial creep relation [2]:

$$e^c = K \sigma t^m \tag{45}$$

in which $K = 29.1 \times 10^{-8}$ and $m = 0.36$ for the temperature at 70°F. The material constants are selected so that the relation closely approximates the family of constant tension creep curves for the type of material under consideration. The modulus of elasticity and Poisson's ratio are E = 442,000 psi and $\nu = 0.3$.

As time goes on, the creep strain at a point within the shell structure under the prescribed loading condition will

progress according to the state of variable increasing stress. By nature of the assumed nonlinearity between creep strain and time function, and for the purpose of comparisons, both strain-hardening and time-hardening approaches are used to obtain solutions. For solutions to be more reliable, only the exact forms of both approaches are selected in the computation.

Perfect Spherical Cap Solutions

Creep buckling analysis is performed for the aforementioned spherical cap model for different uniform pressure levels. In each stress level case, 12 evenly spaced nodal points along the shell surface and 9 across the thickness are selected in the calculation; a Simpson's rule is used for the numerical integration to obtain effective creep loads.

A judicious choice of the time step is critically important in numerical creep solutions. This may be demonstrated in Fig. 6 where the time to collapse for the shell model under 26 psi according to strain-hardening rule is plotted as a function of the time step used in the computation. It is obvious from this figure that the results obtained are highly sensitive to the calculation time step. In the present study, the appropriate time step for a given loading situation is selected from the smaller time step region of collapse time vs time step curve (for example, Fig. 6), so that the difference between the collapse times based on this selected time step and one-half of this step is of minor significance.

The large deformation creep responses (apex displacement vs time) based on both strain-hardening and time-hardening rules are displayed in Figs. 7, 8 and 9, respectively, for pressure levels of 20, 22 and 24 psi. Substantial differences in the creep deformation and the collapse time between both rules are observed for all three cases. In each case, the time-hardening solution predicts a collapse time approximately twice as much as that of the strain-hardening rule. The reason for this is probably due to the nature of development of both rules as has been clearly demonstrated in Fig. 3.

When compared with experimental results as will be made later on in this section, strain-hardening gives a better prediction than time-hardening; the same observation is also found in Ref. [5]. Because of this shortcoming, the time-hardening rule will be excluded from future considerations in this study.

Figure 10 presents a buckling pressure vs collapse time curve (based on strain-hardening) for the shell model considered herein, which shows that the shell buckling pressure decreases with an increase of the collapse time. In other terms, it may be interpreted as that the longer the shell structure lasts, the smaller the buckling pressure is to be anticipated.

Also shown in Fig. 10 is the result (straight broken lines) obtained by assuming the spherical cap to remain free from the creep effect throughout the entire analysis. In

general, the degree of sensitivity of the spherical cap to the creep effect is proportional to the degree of the buckling pressure vs collapse time curve staying away from the straightline solution.

The significance of results shown in Fig. 10 may be extended to other structures. As a matter of practicality that the materials of general structures possess a certain degree of creep behavior, a determination of service loads for a structure should, among others, take the creep behavior and the anticipated structure life into considerations. At any rate, constructions of this type of buckling pressure vs collapse time curves should provide very useful informations for practical designs.

Imperfect Spherical Cap Solutions

Considering the practicality of manufacturing techniques, it is quite hard, if not impossible, to avoid any degree of deviation from the ideal geometrical configuration in a structure. The initial imperfection so induced has been regarded as a major factor to lower the load-carrying capacity for shell structures. Here, we shall examine how the initial imperfection affects the collapse time for the shell model considered herein. The examination may help explain the discrepancy between experimental data and perfect spherical cap solutions.

A dimple type of the axisymmetric imperfection [14,19] is

arbitrarily adopted here, which, nevertheless, does provides a quite adequate description for actual shells since the important parameter is the maximum eccentricity and not the imperfection shape function itself. The adopted imperfection may be expressed mathematically as

$$w_i = (W_{i0}/h)(1 - x^2)^3 \tag{46}$$

where W_{i0} is the maximum imperfection which occurs at the shell apex.

Figures 11, 12 and 13 show the results in the form of collapse time vs maximum imperfection magnitude for the shell model under pressures of 20, 22, 24 psi, respectively. It is surprising to find from these results that initial imperfections have such a profound impact on shortening the shell life. For example, with a $W_{i0}/h = 0.06$, which, in effect, is sometimes very hard to be measured accurately and may be regarded too small to be significant, the corresponding shell lifes in these cases are less than 1/3 of those for the perfect shells. By showing such a high degree of sensitivity of the collapse time to the initial imperfection, results obtained strongly suggest that the presence of initial imperfections must be fully taken into consideration in any creep analysis before such analysis can be expected to accurately estimate the collapse time of practical shell structures.

Comparison With Test Results

As already mentioned at the beginning of this section, the shell models selected for investigation in this study were originally manufactured in Ref. [2]. The creep data were obtained from constant stress tests, and the mathematical model, Eq. (45), fitted to the creep curves was also proposed in this reference. Experiments were performed for three different pressure levels of 20, 22, and 24 psi, and, at each pressure level, the center displacement was recorded continuously for five separate test shells. Experimental results in terms of the apex displacement history are displayed in Figs. 14, 15, and 16 for pressure levels of 20, 22, and 24 psi, respectively. Also displayed in these Figures are present theoretical solutions for the same shell model with and without initial imperfections.

If comparisons are made between experimental data and perfect spherical cap solutions, it is evident that a huge discrepancy exists between them in both creep deformation and collapse time. The discrepancy has to be at least in part attributed to initial imperfections which, according to the claims made in Ref. [2], is resulted from the fact that the measured data showing that the test shells are not perfectly spherical even if the deviation from sphericity is small. Another factor also contributing to this discrepancy is related to the validity of the mathematical model used to describe the creep behavior.

Now, we turn our attention to the comparison between experimental data and theoretical results for the imperfect spherical caps, noting that, in each pressure level case, a number of theoretical solutions associated with imperfection magnitudes ranging from 0 to 0.1 are displayed in the figures. To be more specific, comparisons should be focused on two different aspects, namely, the collapse time and the center deflection history.

Of course, for the comparison to be completely satisfactory, good agreements should be achieved simultaneously on these two aspects. Unfortunately, results displayed in these figures show that good agreement can only be obtained for either the collapse time or the deflection history, not both at the same time. For example, in Fig. 14, the entire theoretical deflection history for $W_{io}/h = 0.1$ (curve AB) agrees almost completely with that of experiment (curve ABC), but the theory predicts a much shorter collapse time than the experiment. On the other hand, the theory associated $W_{io}/h = 0.06$ yields a good prediction on the collapse time but a poor estimate on the creep deformation when compared with experimental curve AD.

It is interesting to note that, in the case of $W_{i0}/h = 0.1$ of Fig. 14, theoretical deflection curve AB is only a part of experimental curve ABC. When these two curves are compared with the sketch of the general creep behavior (Fig. 2), it may suffice to say that the present mathematical

creep model, Eq. (45), is valid only up to the secondary stage of creep, and that the difference between these two curves, Curve BC, is related to the tertiary creep which obviously is not implemented in the present creep model.

We may sum up all the discussion here by stating that, for the shell models considered herein, in order to have a completely satisfactory comparison with experimental data, the theoretical analysis should fully take the presence of initial imperfections into consideration, and should also adopt a mathematical creep model which includes not only the primary and the secondary creep but the tertiary creep.

CONCLUSIONS

A numerical procedure has been developed for the large deformation creep buckling analysis of axisymmetric spherical caps. The problem formulation is based on governing differential equations, treating creep deformations as effective creep loads which are combined with actual applied forces. The shell models selected for the present analysis are simply supported, uniformly loaded spherical caps, made of Type 6/6 Nylon and previously tested in Ref. [2]. A nonlinear mathematical creep model proposed in Ref. [2] is adopted in the present analysis, which closely approximates the family of constant stress tension creep curves.

For the nonlinear creep analysis, both strain-hardening and time-hardening rules are employed. Results obtained in-

dicate that, when compared with experimental data, strain-hardening provides better predictions on collapse time than time-hardening, and that they are highly sensitive to the calculation time step that a jucicious choice of this value is essential to their accuracy.

In Fig. 10, the buckling pressure is plotted as a function of the collapse time for the shell model considered herein, which shows that the shell buckling pressure decreases with an increase of collapse time. In other words, for a structure which displays a significant creep behavior at the given temperature, the longer the structure life, the smaller the load-carrying capacity. Construction of this type of buckling pressure vs collapse time curves should provide very useful information for the purpose of practical designs.

The present theoretical solutions for the perfect spherical cap models predict very poorly for both creep deflections and collapse time when compared with experimental data. The poor theoretical predictions have to be attributed primarily to initial imperfections which, according to the measured data in Ref. [2], are resulted from deviations from the sphericity of test specimens. On the other hand, results of imperfect spherical caps indicate that, with very small magnitude of imperfections introduced in the shell models, theoretical predictions are improved substantially.

Two important points are noted here. First, the collapse time of the shell models is very sensitive to initial

imperfections as can be seen from Figs. 11, 12, and 13. For example, with a maximum imperfection magnitude of W_{i0}/h equal to only 0.06, the collapse time of imperfect shell models is only about 1/3 of perfect shell values. Second, for an adequate imperfection magnitude, good agreement between theoretical and experiment results can only be obtained for either the collapse time or the creep deformation, not both at the same time. A careful examination on the course of this shortcoming reveals that, in order to have a completely satisfactory comparison with experimental data, in addition to fully taking into account the presence of initial imperfections, the theoretical analysis should adopt a mathematical creep model which includes not only the primary and the secondary creep but also the tertiary creep.

REFERENCES

[1] Hoff, N. J., "A survey of the theories of creep buckling," Proceedings of the Third U. S. National Congress of Applied Mechanics, ASME, New York, 1958, p. 20.

[2] Shi, J., Johnson, C. D., and Bauld, N. R., Jr., "Application of the variational theorem for creep of shallow spherical shells," AIAA Journal, Vol. 8, No. 3, March 1970.

[3] Lin, T. H., Theory of Inelastic Structures, John Wiley and Sons, Inc., New York, 1968.

[4] Odqvist, F. K. G., Mathematical Theory of Creep and Creep Rupture, Oxford at the Clarendon Press, 1974.

[5] Finnie, I., and Heller, W. R., Creep of Engineering Materials, McGraw-Hill Co., Inc., New York, 1959.

[6] Pao, Y. H. and Martin, J., An analytical theory of the creep deformation of materials, Trans. Am. Soc. Mech. Engrs., J. Appl. Mech. 20, 245-252 (1953).

[7] Diamant, E. S., "Axisymmetric creep in cylindrical shells," AIAA Journal, Vol. 5, No. 10, October 1967.

[8] Kao, R., "A note on buckling of spherical caps with initial asymmetric imperfections," J. Appl. Mech. 39(3) Series E, Sept. 1972.

[9] Kao, R., and Perrone, N., "Dynamic buckling of axisymmetric spherical caps with initial imperfections," Computers and Structures, Vol. 9, pp. 463-473, 1978.

[10] Kao, R., "A comparative study on the elastic-plastic collapse strength of initially imperfect deep spherical shells," to appear in International Journal for Numerical Methods in Engineering.

[11] Samuelson, L. A., "Creep buckling of imperfect circular cylindrical shells under non-uniform external loads," Creep in Structures, Symposium Gothenburg (Sweden) Aug. 1970.

[12] Hoff, N. J., "Axially symmetric creep buckling of circular cylindrical shells in axial compression," J. Appl. Mech. 35, Sept. 1968.

[13] Shanley, F., Weight-strength analysis of aircraft structures, McGraw-Hill, New York, 1952.

[14] Kao, R., "Large Deformation Elastic-Plastic Buckling Analysis of Spherical Caps with Initial Imperfections," To appear in Computers and Structures.

[15] Kao, R., "Nonlinear Dynamic Buckling of Spherical Caps with Initial Imperfections," To appear in Computers and Structures.

[16] Hill, R., The Mathematical Theory of Plasticity, Oxford Univ. Press, 1950.

[17] Ziegler, H., "A Modification of Prager's Hardening Rule," Quart. Appl. Math., Vol. 17, No., 1959.

[18] Sanders, J. L., McComb, H. G., Jr., and Schlechte, F. R., "A variational theorem for creep with applications to plates and columns," NACA Technical Note 4003, 1957.

[19] Koga, T. and Hoff, N. J., "The Axisymmetric Buckling of Initially Imperfect Complete Spherical Shells," Internal Journal Solids and Structures (July 1969).

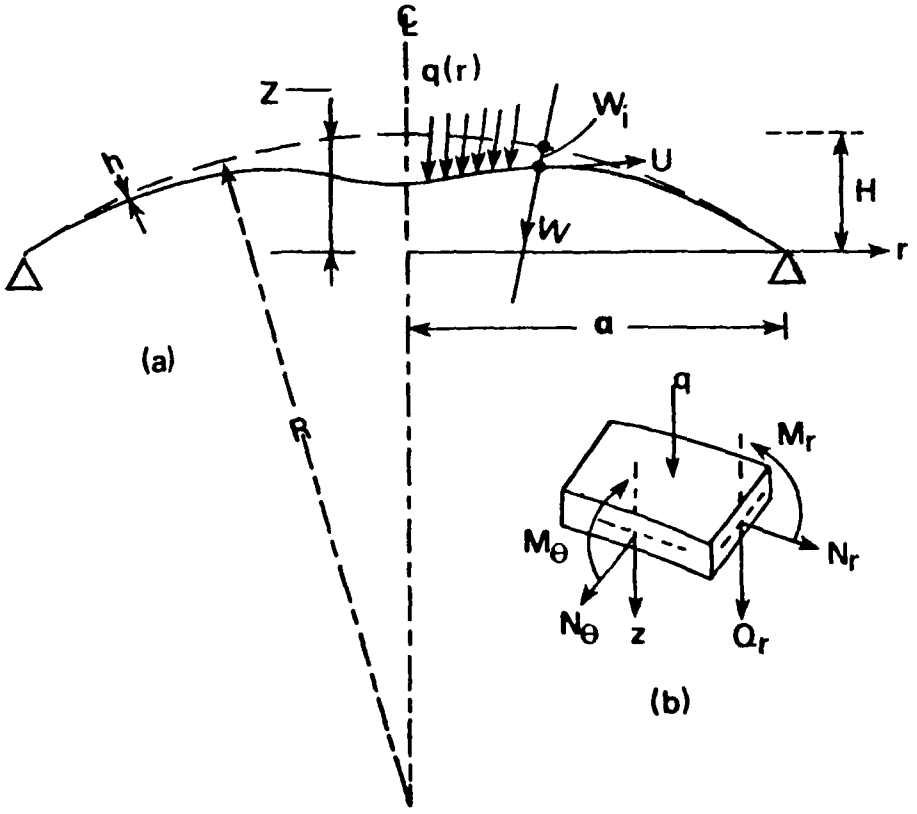

Fig.1 – Geometry, stress resultants and moments for axisymmetric simply supported spherical cap with initial imperfection.

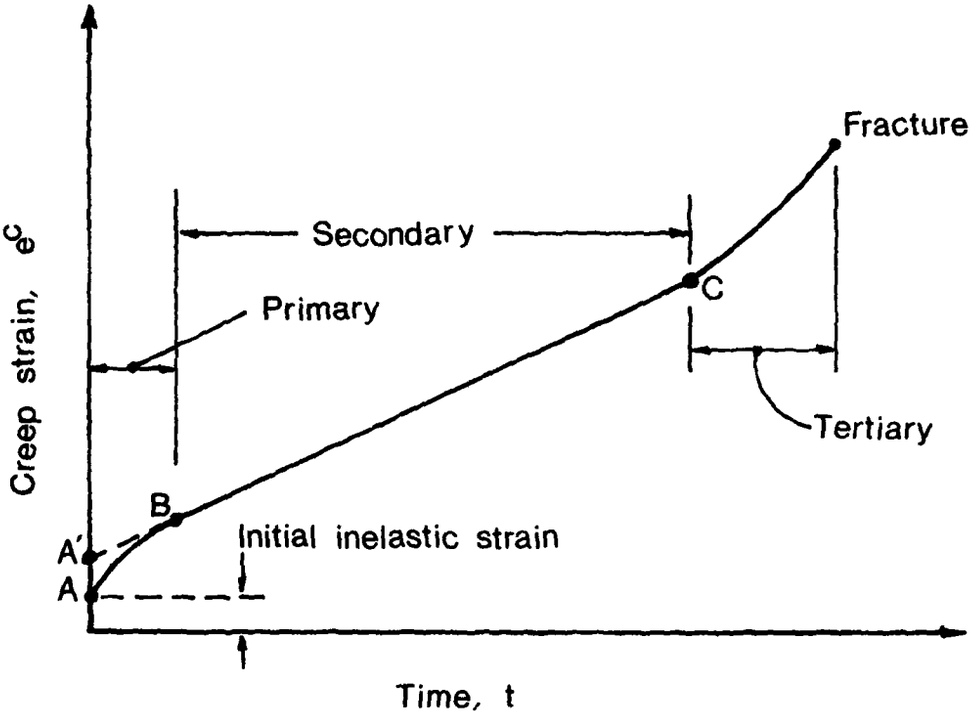

Fig.2 - A typical creep curve under constant stress.

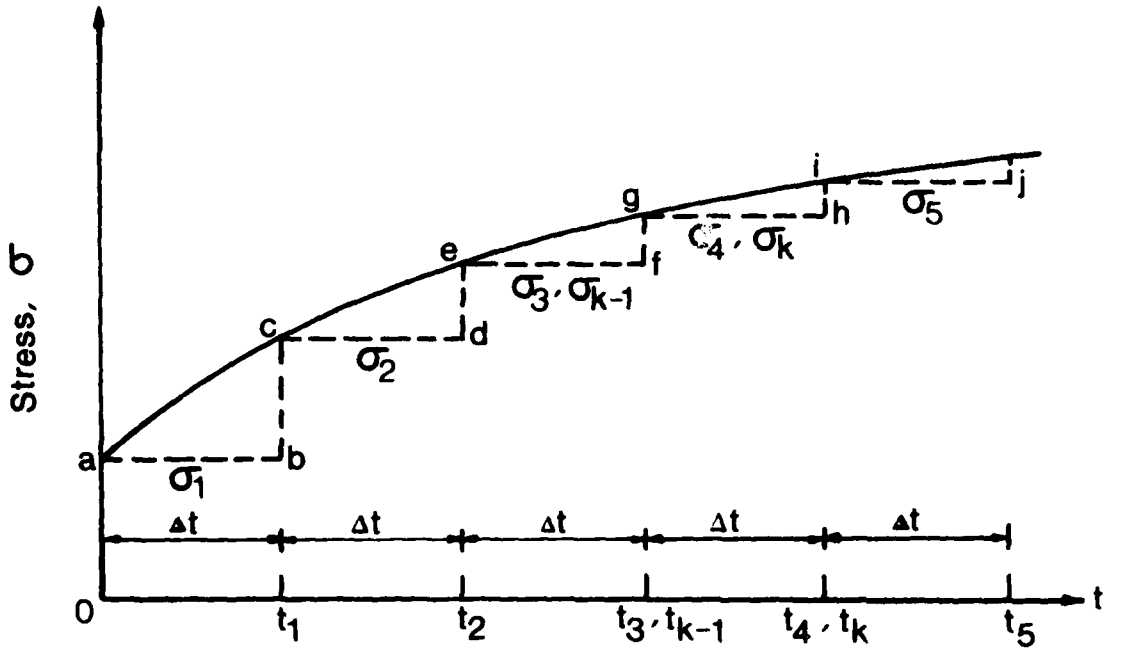
Stress, σ
a
b
c
d
e
f
g
h
i
j
σ1
σ2
σ3 · σk-1
σ4 · σk
σ5
Δt
Δt
Δt
Δt
Δt
0
t1
t2
t3 · tk-1
t4 · tk
t5
t

3(a)

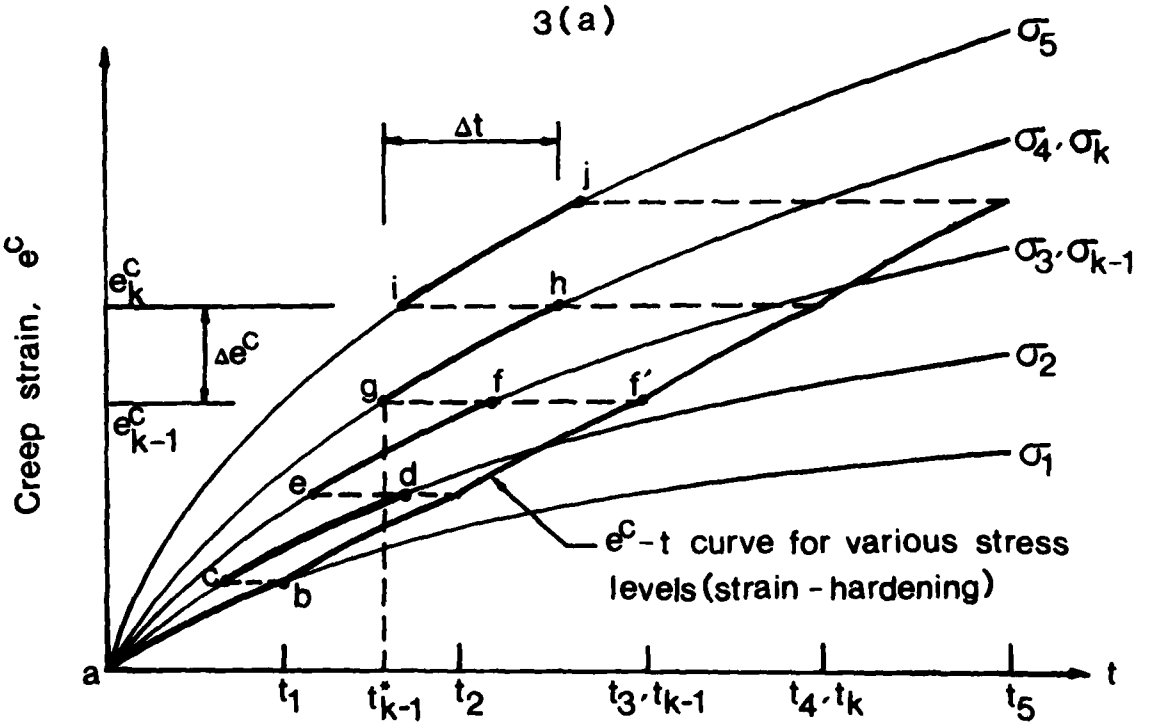
Creep strain, e^c
σ5
σ4 · σk
σ3 · σk-1
σ2
σ1
Δt
j
i
h
g
f
f'
e
d
c
b
a
e^c_k
Δe^c
e^c_k-1
e^c - t curve for various stress levels (strain - hardening)
t1
t*k-1
t2
t3 · tk-1
t4 · tk
t5
t

3(b)

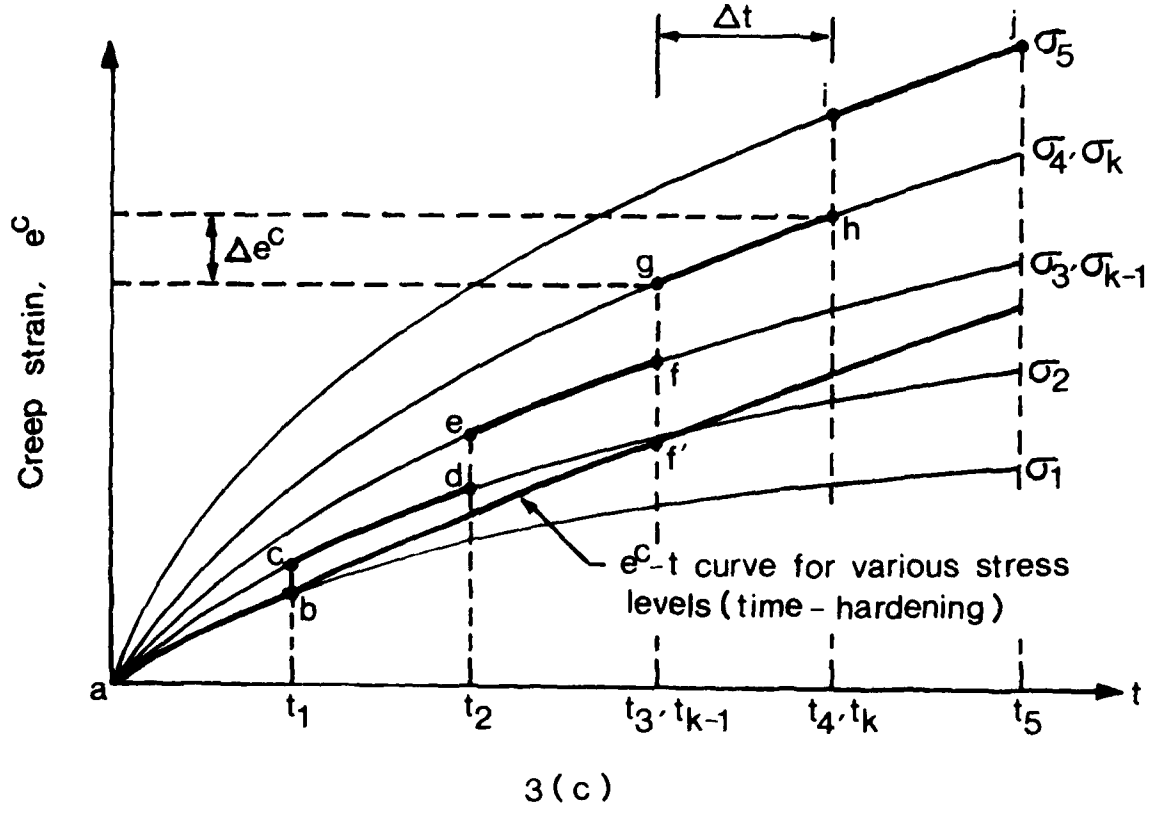

Fig. 3 - (a) Approximation of the smooth stress-time curve by steps, (b) Creep strain-time curve for various stress levels according to strain-hardening rule, (c) Creep strain-time curve for various stress levels according to time-hardening rule.

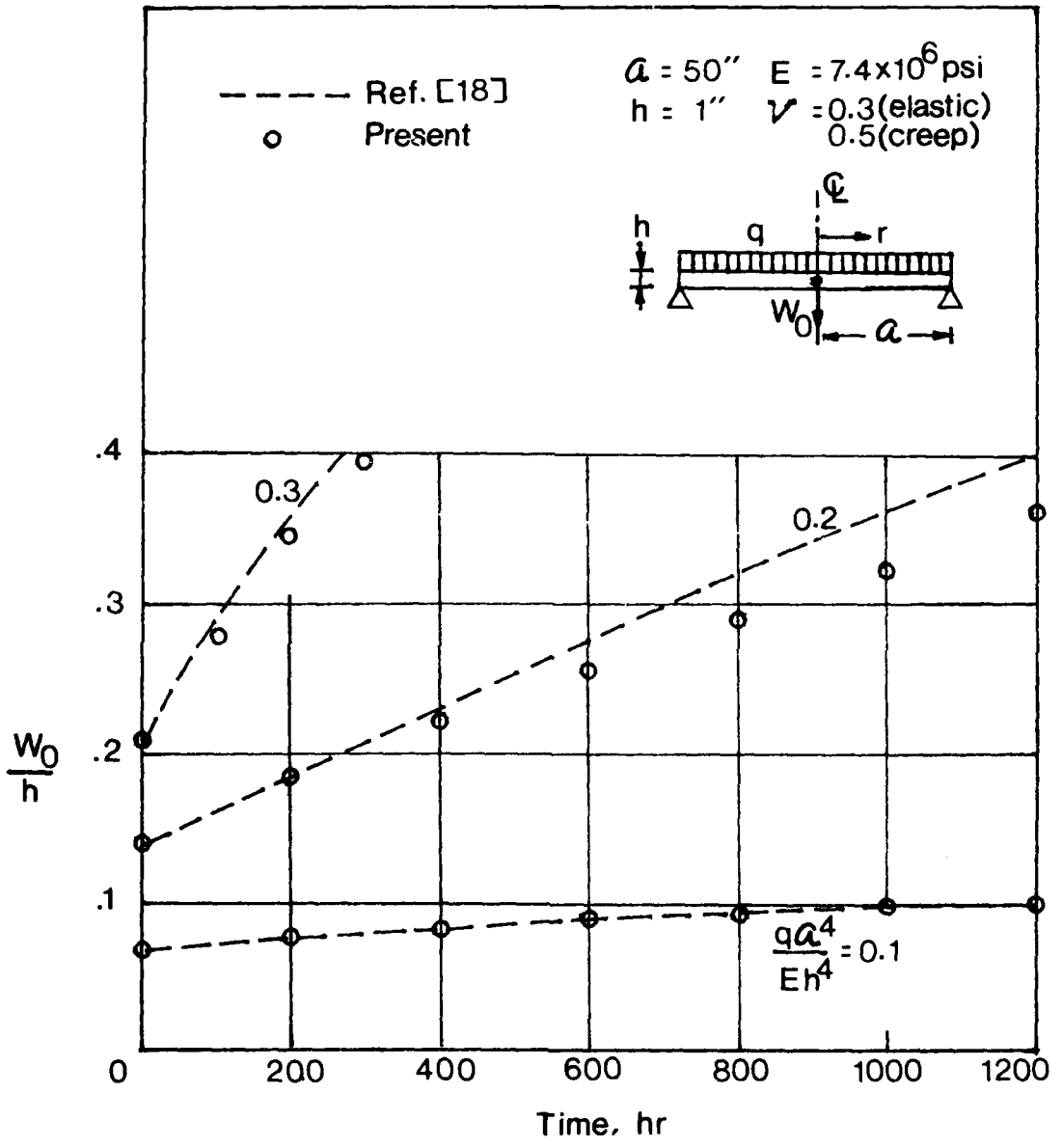

Fig.4 - Center deflection vs time (steady creep response) for a simply supported circular plate under uniform loading; material is 2024 - T3 aluminum alloy at 600°F.

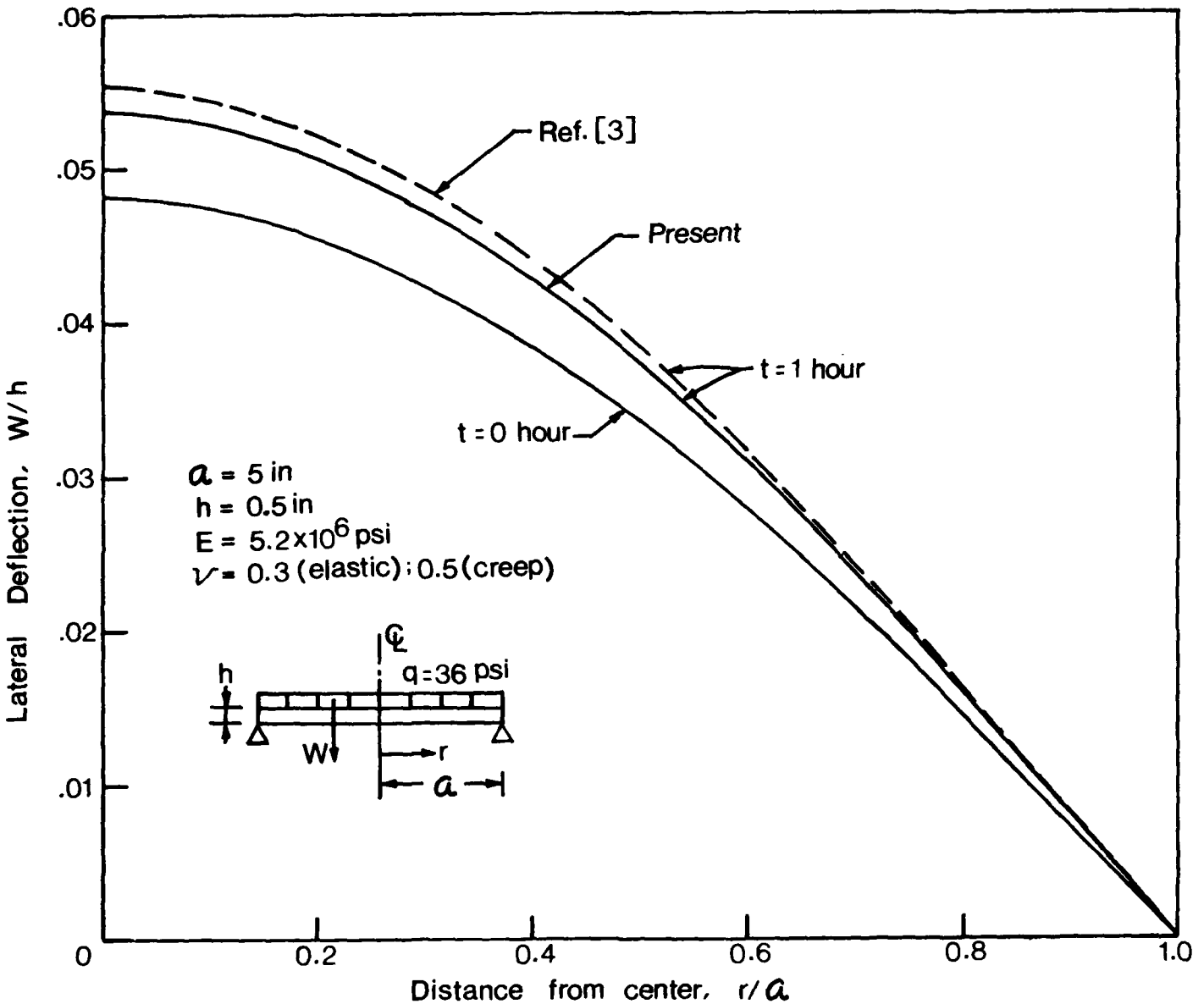

Fig. 5 - Deflection profile (primary creep response) for a uniformly loaded, simply supported circular plate of 75ST aluminum alloy at 600°F.

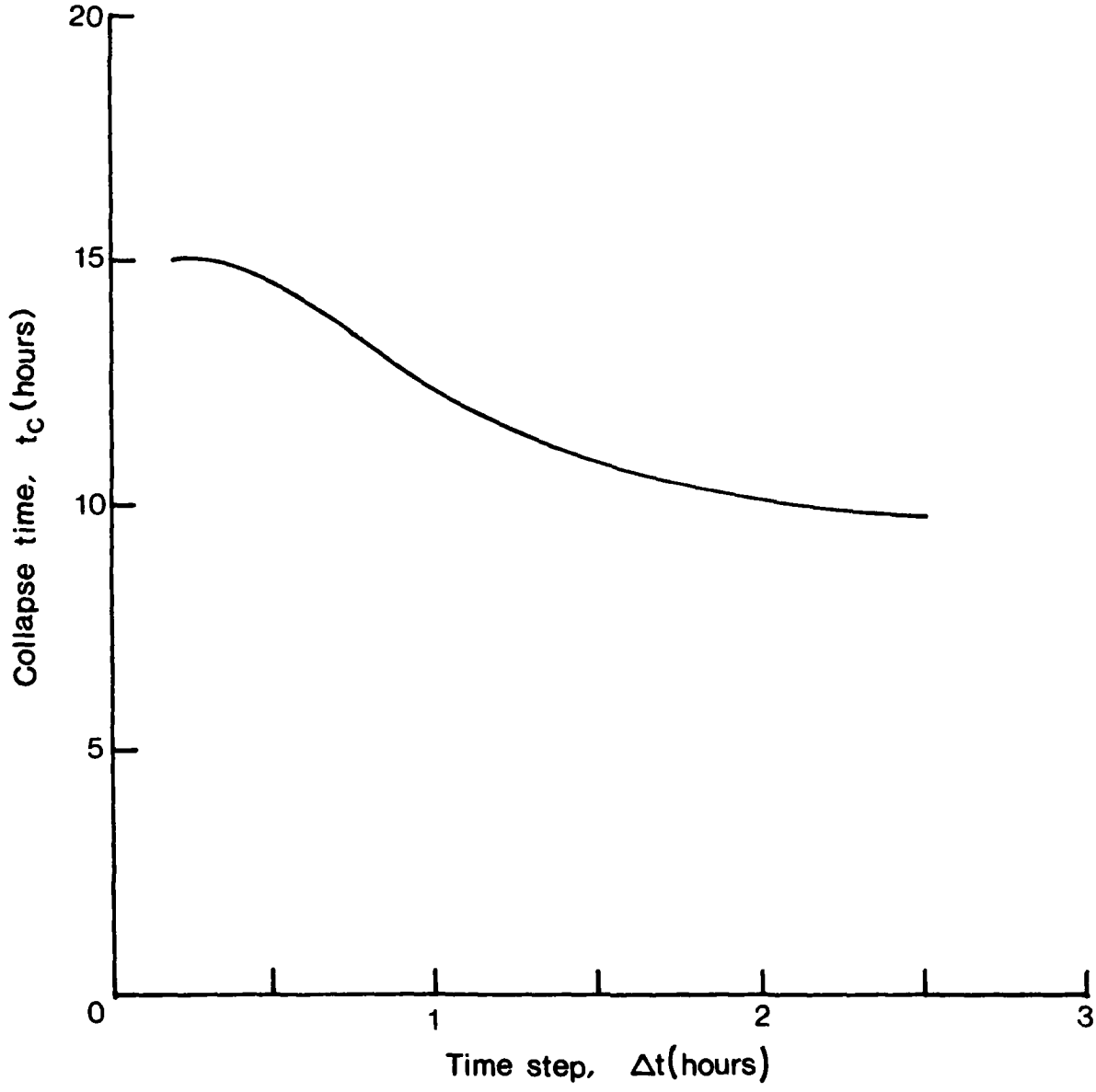

Fig. 6 - Effect of time step in calculation of collapse time (strain hardening) for a spherical cap model under uniform pressure of 26 psi.

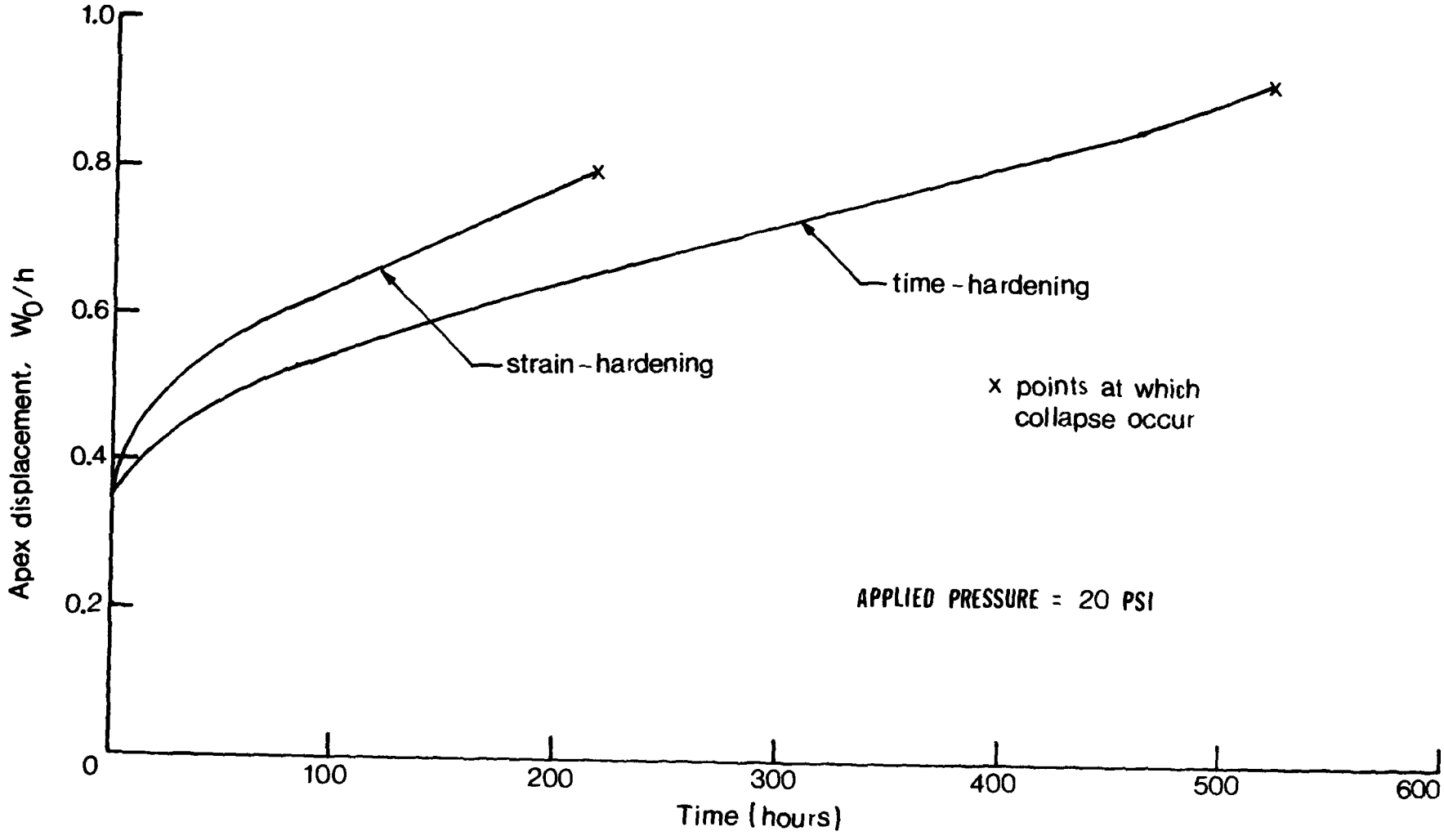

Fig. 7 - Large deformation creep response for a spherical cap model under uniform pressure of 20 psi.

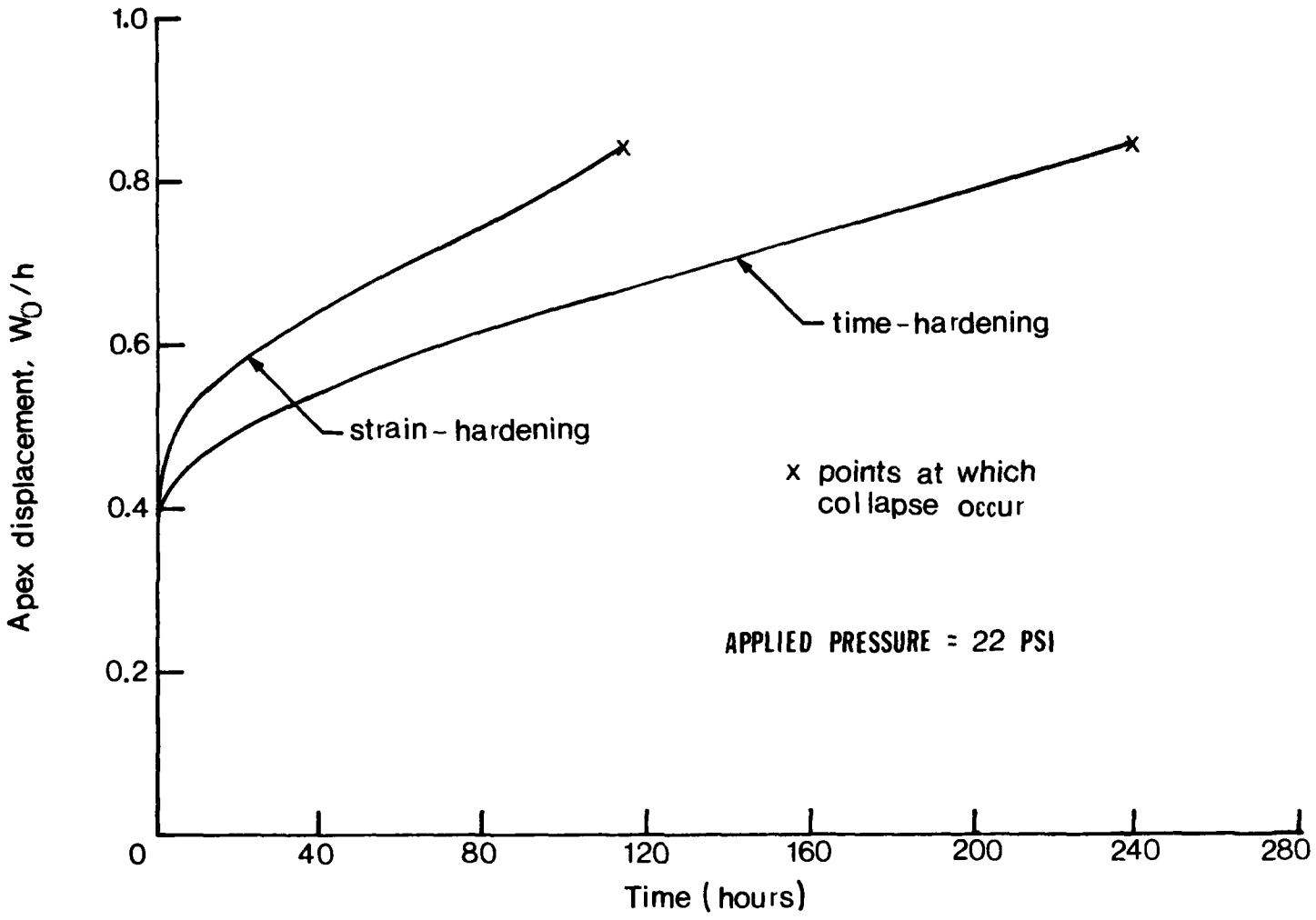

Fig. 8 - Large deformation creep response for a spherical cap model under uniform pressure of 22 psi.

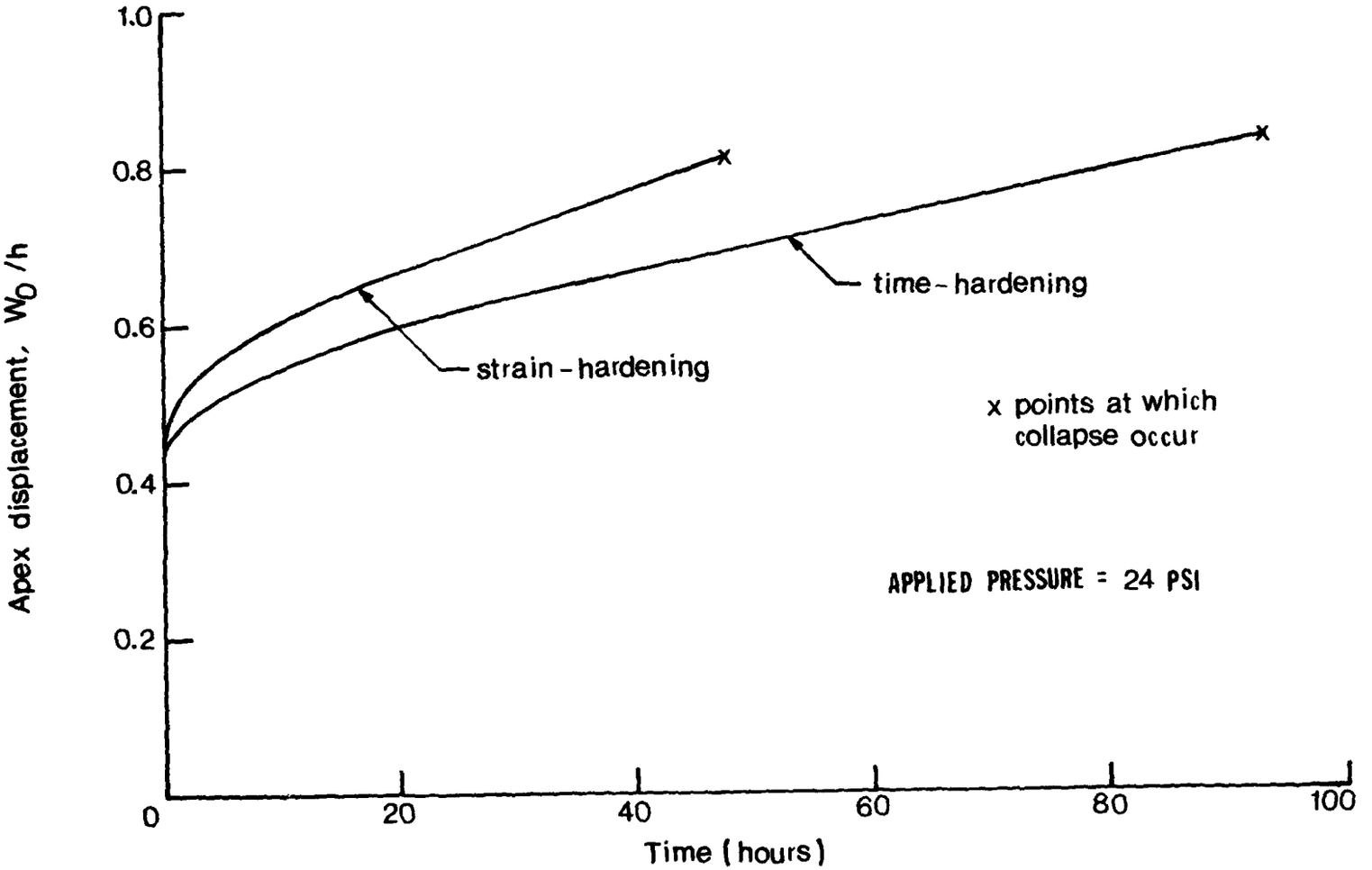

Fig. 9 Large deformation creep response for a spherical cap model under uniform pressure of 24 psi.

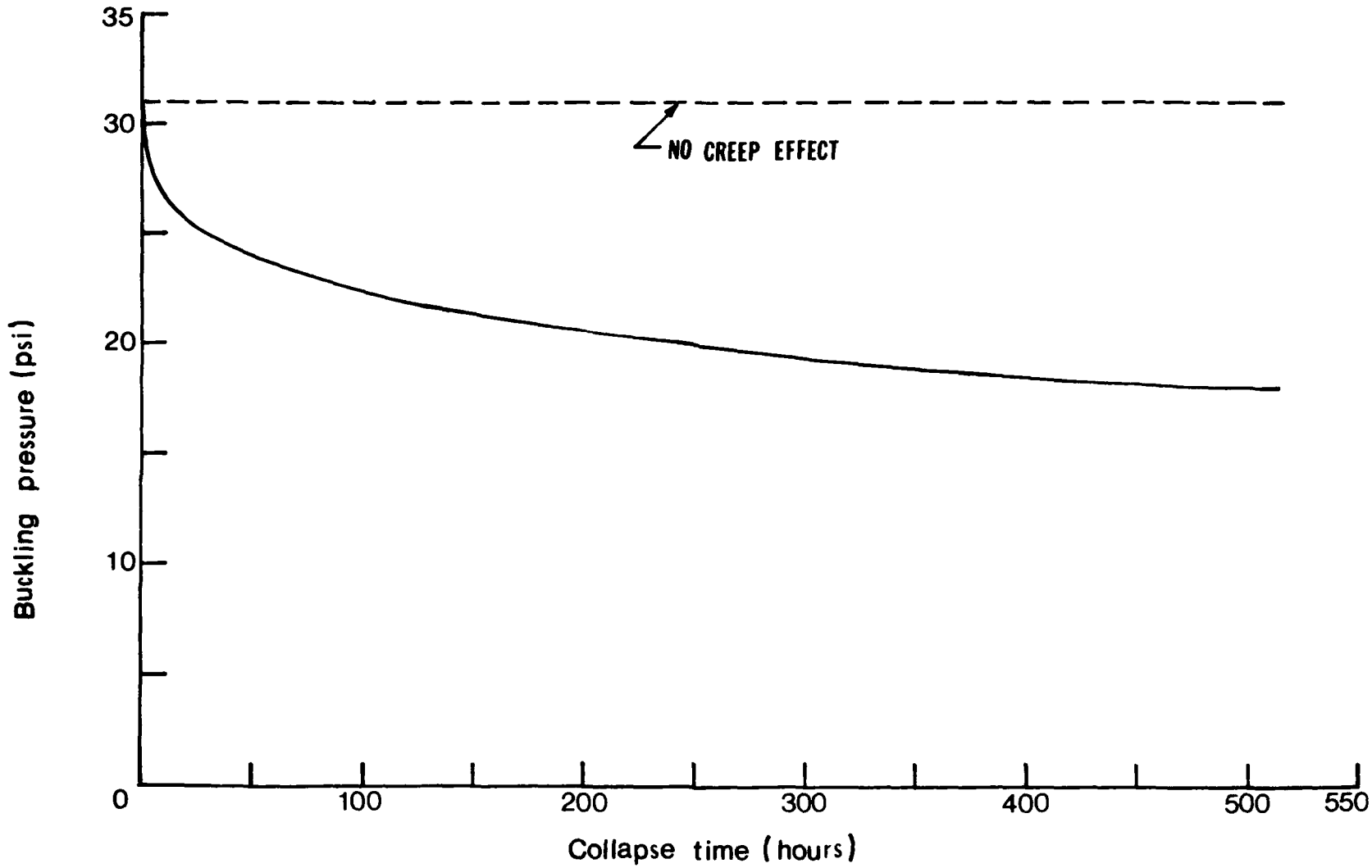

Fig 10- Buckling pressure vs collapse time for a uniformly loaded, simply supported spherical cap model.

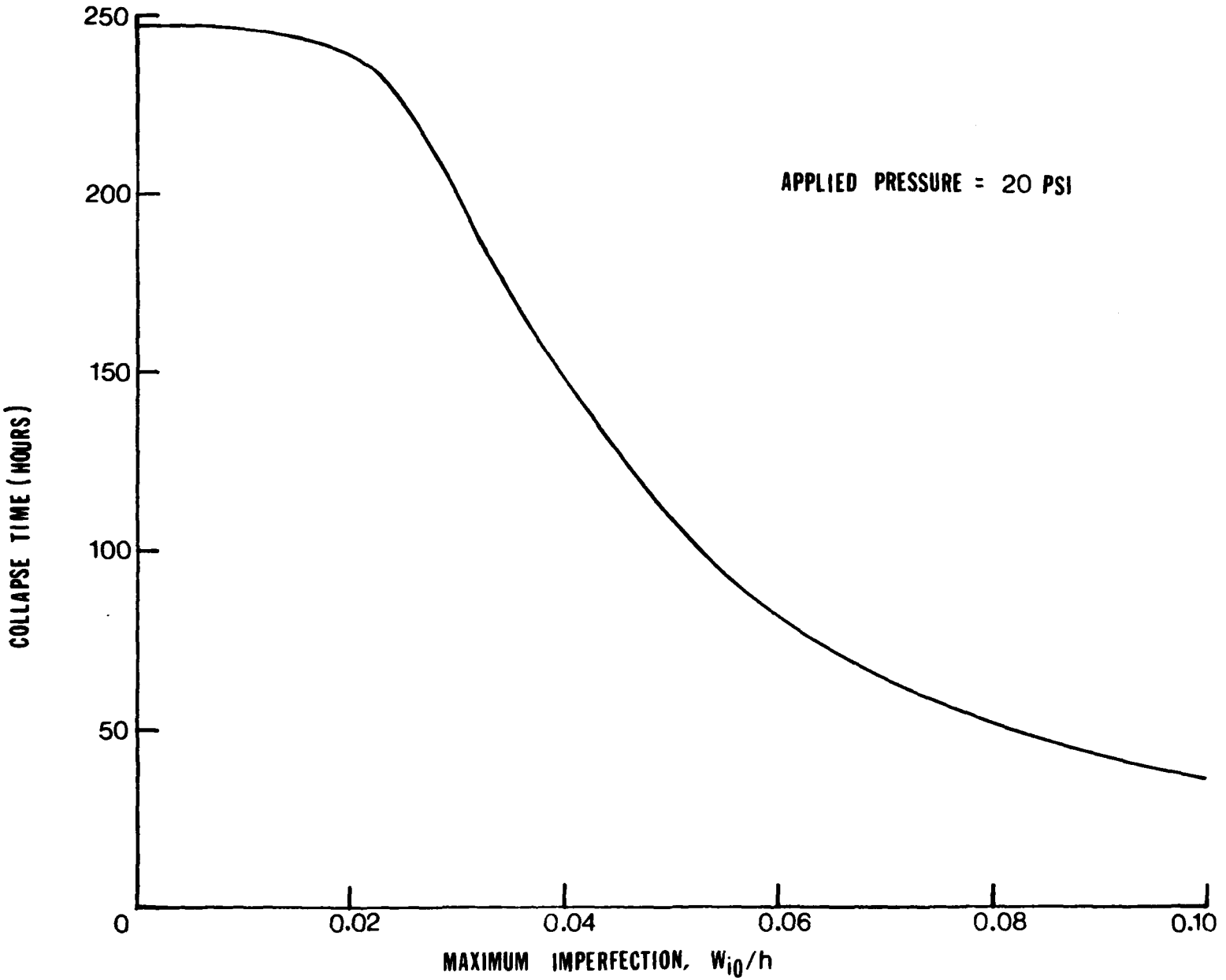

FIG. 11 – COLLAPSE TIME VS INITIAL IMPERFECTION FOR A SIMPLY SUPPORTED SPHERICAL CAP MODEL UNDER UNIFORM PRESSURE OF 20 PSI.

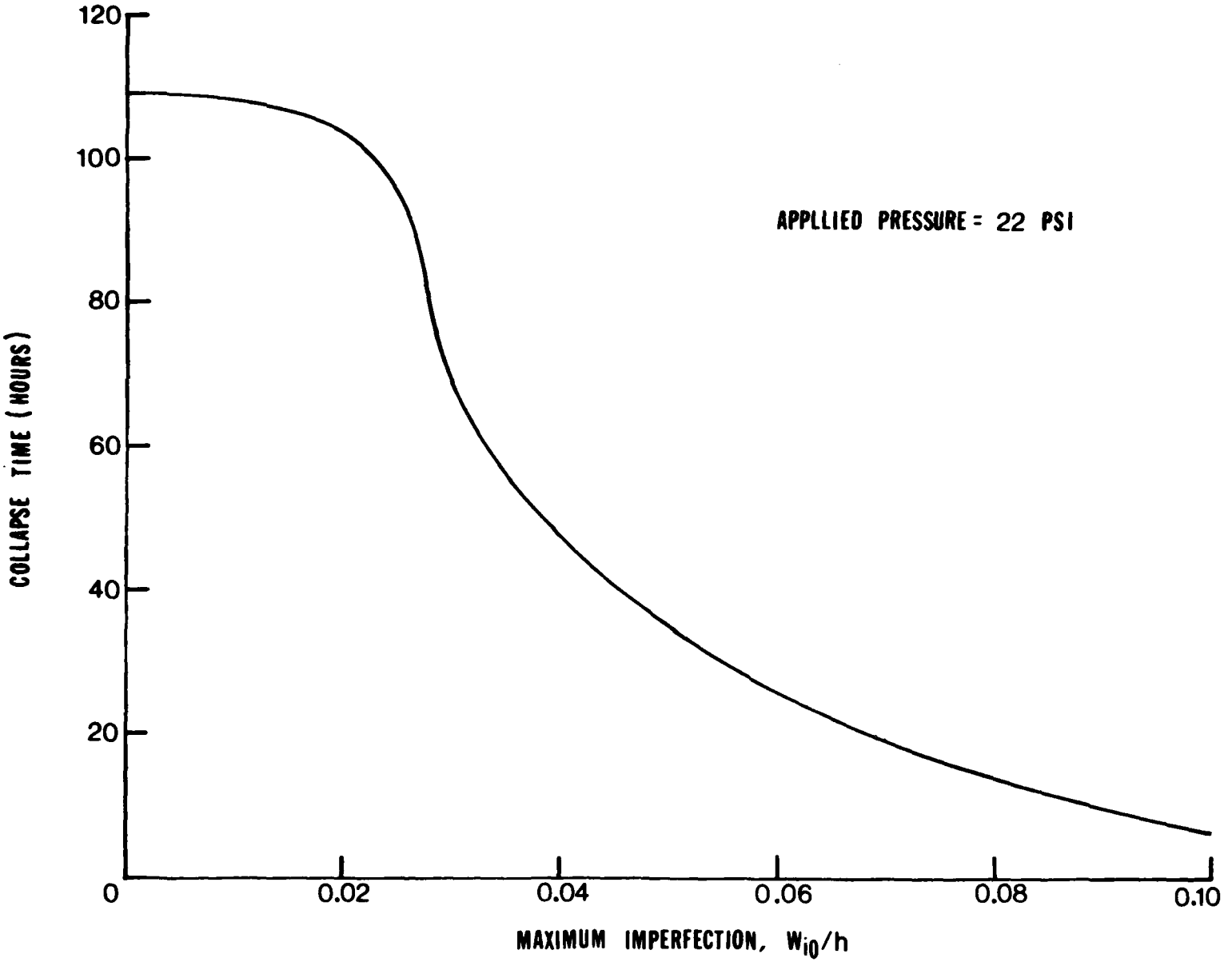

FIG. 12 - COLLAPSE TIME VS INITIAL IMPERFECTION FOR A SIMPLY SUPPORTED SPHERICAL CAP MODEL UNDER UNIFORM PRESSURE OF 22 PSI.

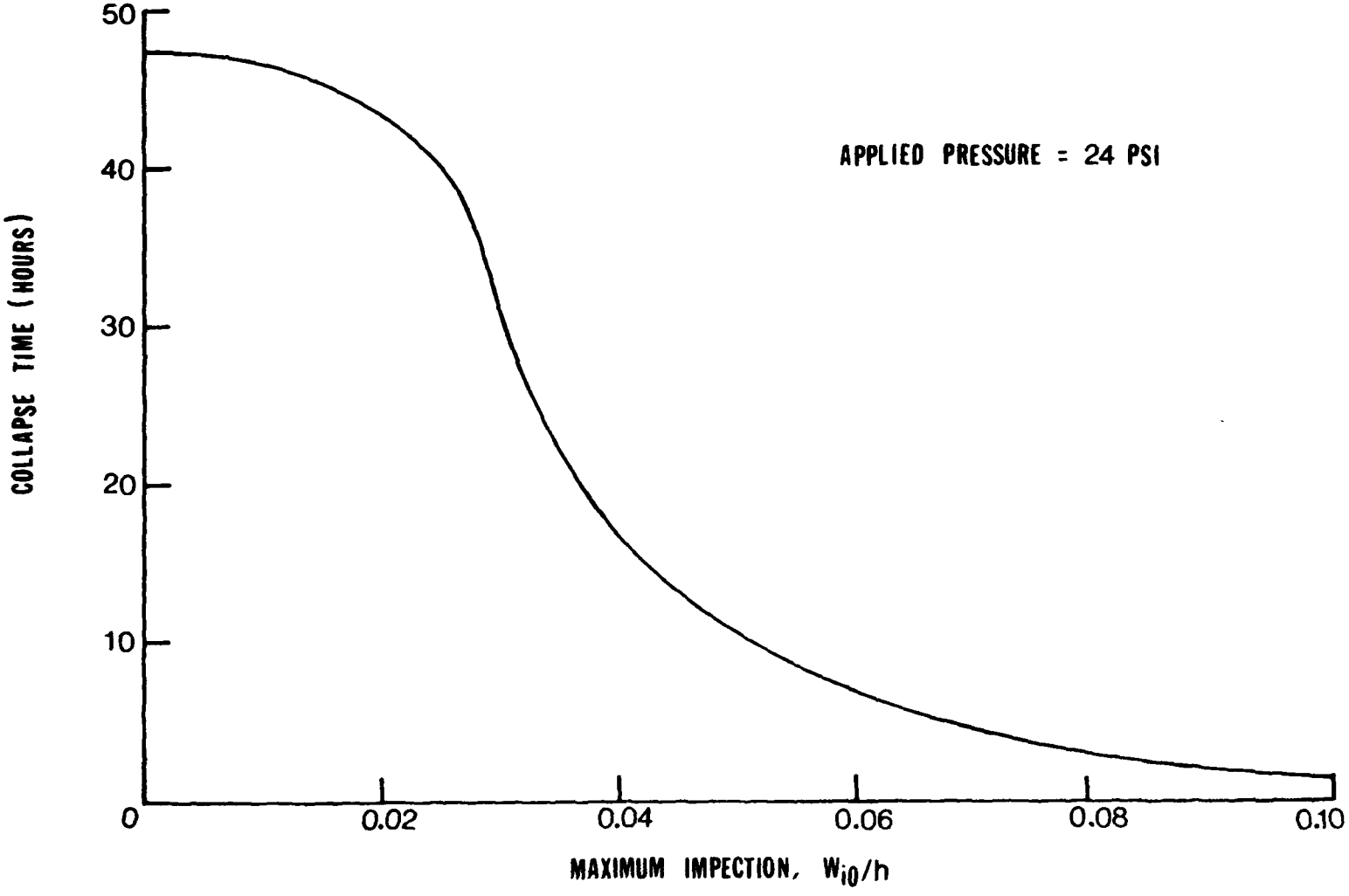

FIG. 13 - COLLAPSE TIME VS INITIAL IMPERFECTION FOR A SIMPLY SUPPORTED SPHERICAL CAP MODEL UNDER UNIFORM PRESSURE OF 24 PSI.

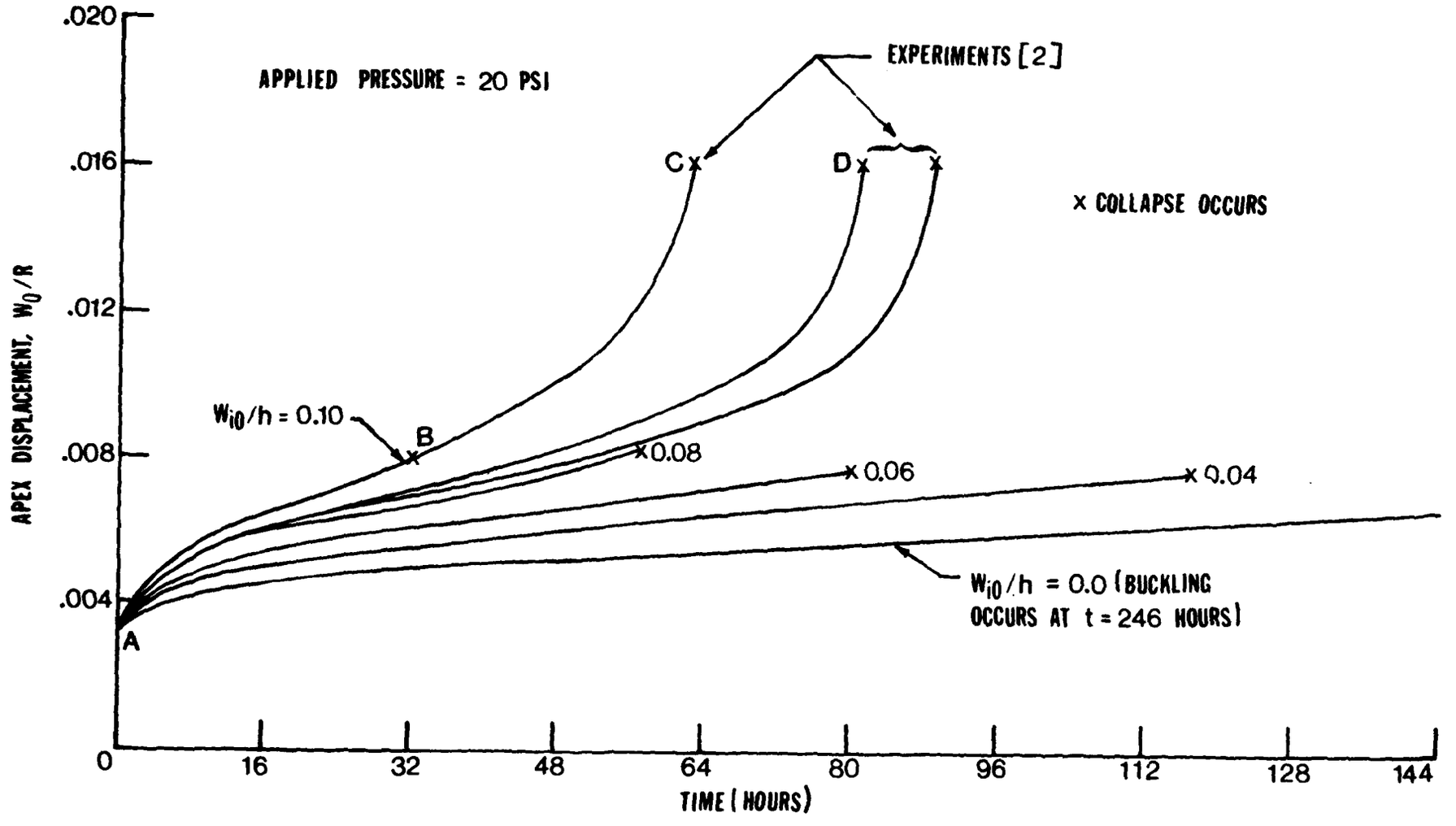

FIG. 14 – COMPARISON OF CREEP BUCKLING RESPONSE FOR A SPHERICAL CAP MODEL UNDER UNIFORM PRESSURE OF 20 PSI.

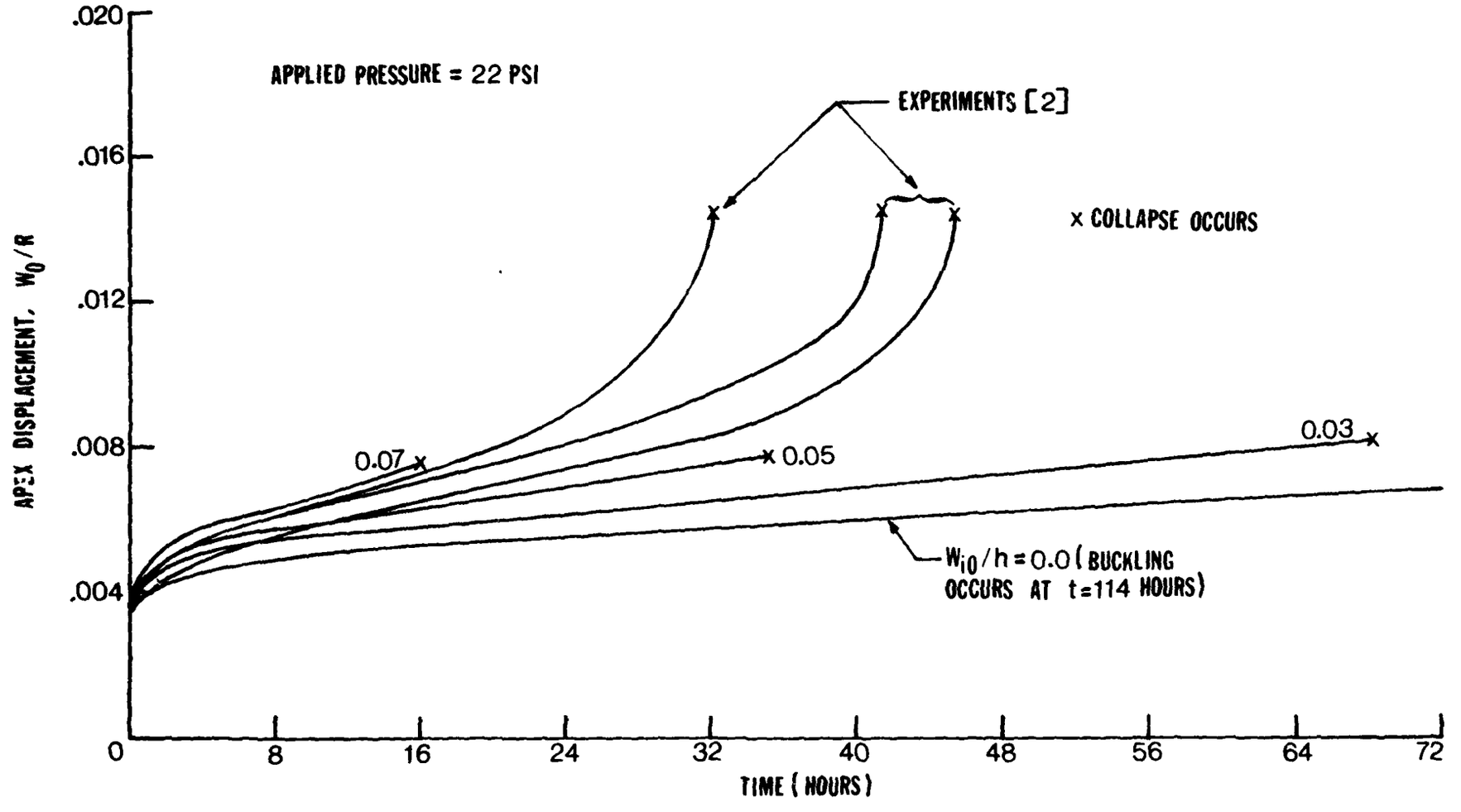

FIG. 15 – COMPARISON OF CREEP BUCKLING RESPONSE FOR A SPHERICAL CAP MODEL UNDER UNIFORM PRESSURE OF 22 PSI.

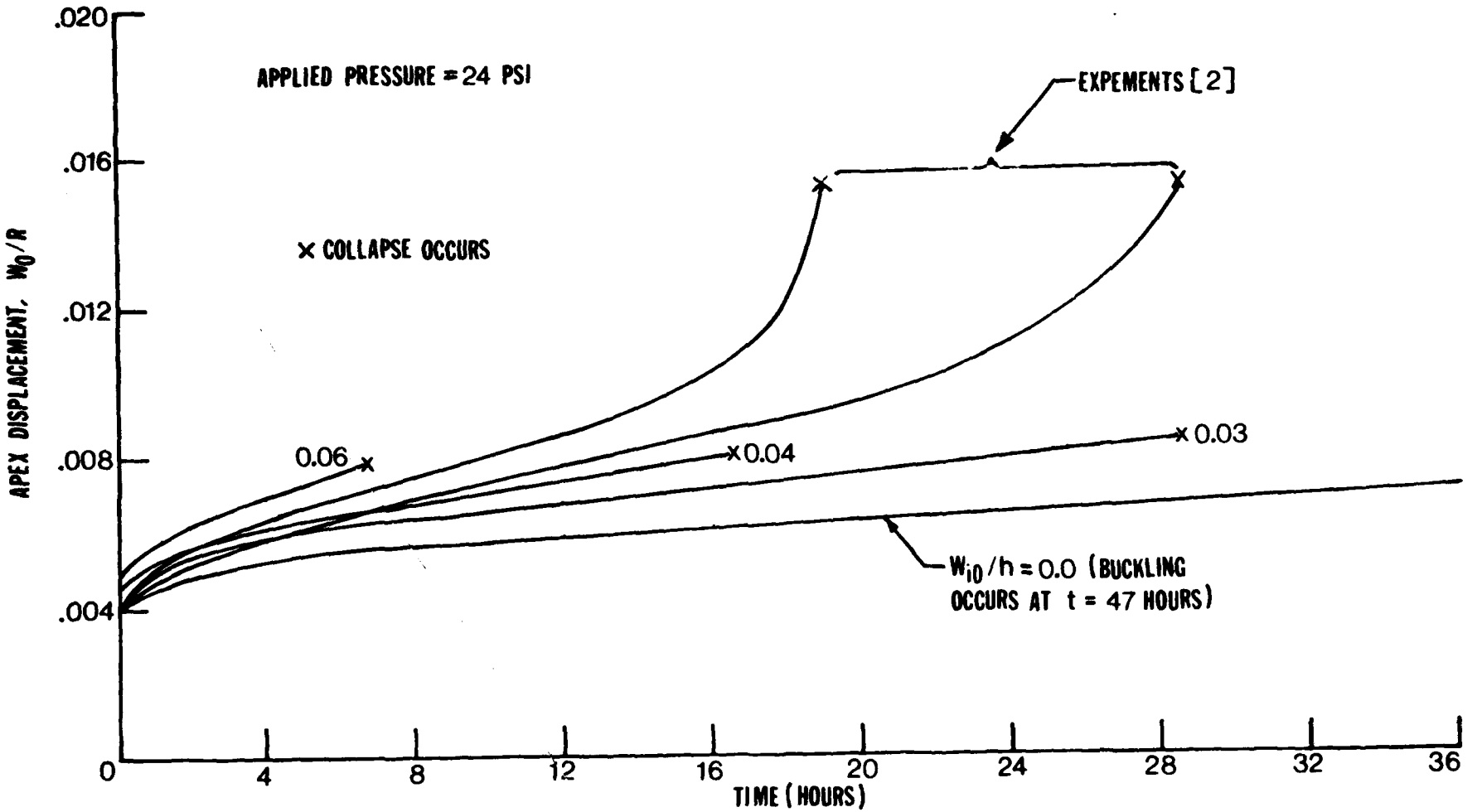

FIG. 16 – COMPARISON OF CREEP BUCKLING RESPONSE FOR A SPHERICAL CAP MODEL UNDER UNIFORM PRESSURE OF 24 PSI.

SECURITY CLASSIFICATION OF THIS PAGE (When Data Entered)

REPORT DOCUMENTATION PAGE	READ INSTRUCTIONS BEFORE COMPLETING FORM
1. REPORT NUMBER	2. GOVT ACCESSION NO. AD-A087 017 / 3. RECIPIENT'S CATALOG NUMBER
4. NONLINEAR CREEP BUCKLING ANALYSIS OF INITIALLY IMPERFECT SHALLOW SPHERICAL SHELLS	5. TYPE OF REPORT & PERIOD COVERED 6. PERFORMING ORG. REPORT NUMBER
7. AUTHOR(s) Robert Kao	8. CONTRACT OR GRANT NUMBER(s) NAVY 00014-75-C-0946
9. PERFORMING ORGANIZATION NAME AND ADDRESS The George Washington University School of Engineering and Applied Science Washington, D.C. 20052	10. PROGRAM ELEMENT, PROJECT, TASK AREA & WORK UNIT NUMBERS
11. CONTROLLING OFFICE NAME AND ADDRESS Office of Naval Research Arlington, Virginia 22217	12. REPORT DATE July 1980 13. NUMBER OF PAGES 49
14. MONITORING AGENCY NAME & ADDRESS(if different from Controlling Office)	15. SECURITY CLASS. (of this report) 15a. DECLASSIFICATION/DOWNGRADING SCHEDULE

16. DISTRIBUTION STATEMENT (of this Report)

APPROVED FOR PUBLIC RELEASE: DISTRIBUTION UNLIMITED

17. DISTRIBUTION STATEMENT (of the abstract entered in Block 20, if different from Report)

18. SUPPLEMENTARY NOTES

19. KEY WORDS (Continue on reverse side if necessary and identify by block number)

Collapse time	Initial imperfections
Creep deformation	Spherical caps
Large deformation	Finite differences
Strain-hardening	Primary, Steady, Tertiary Creep
Time-hardening	Nonlinear creep

20. ABSTRACT (Continue on reverse side if necessary and identify by block number)

Creep buckling times and creep deformations are obtained for axisymmetric shallow spherical shells with and without initial imperfections. For nonlinear creeps, both strain-hardening and time-hardening rules are employed in the analysis; results indicate that strain-hardening yields better estimates of shell life than time-hardening. Results also show that the initial imperfection plays an important role in shortening shell creep buckling times.

DD FORM 1 JAN 73 1473 EDITION OF 1 NOV 65 IS OBSOLETE

S/N 0102-014-6601

SECURITY CLASSIFICATION OF THIS PAGE (When Data Entered)

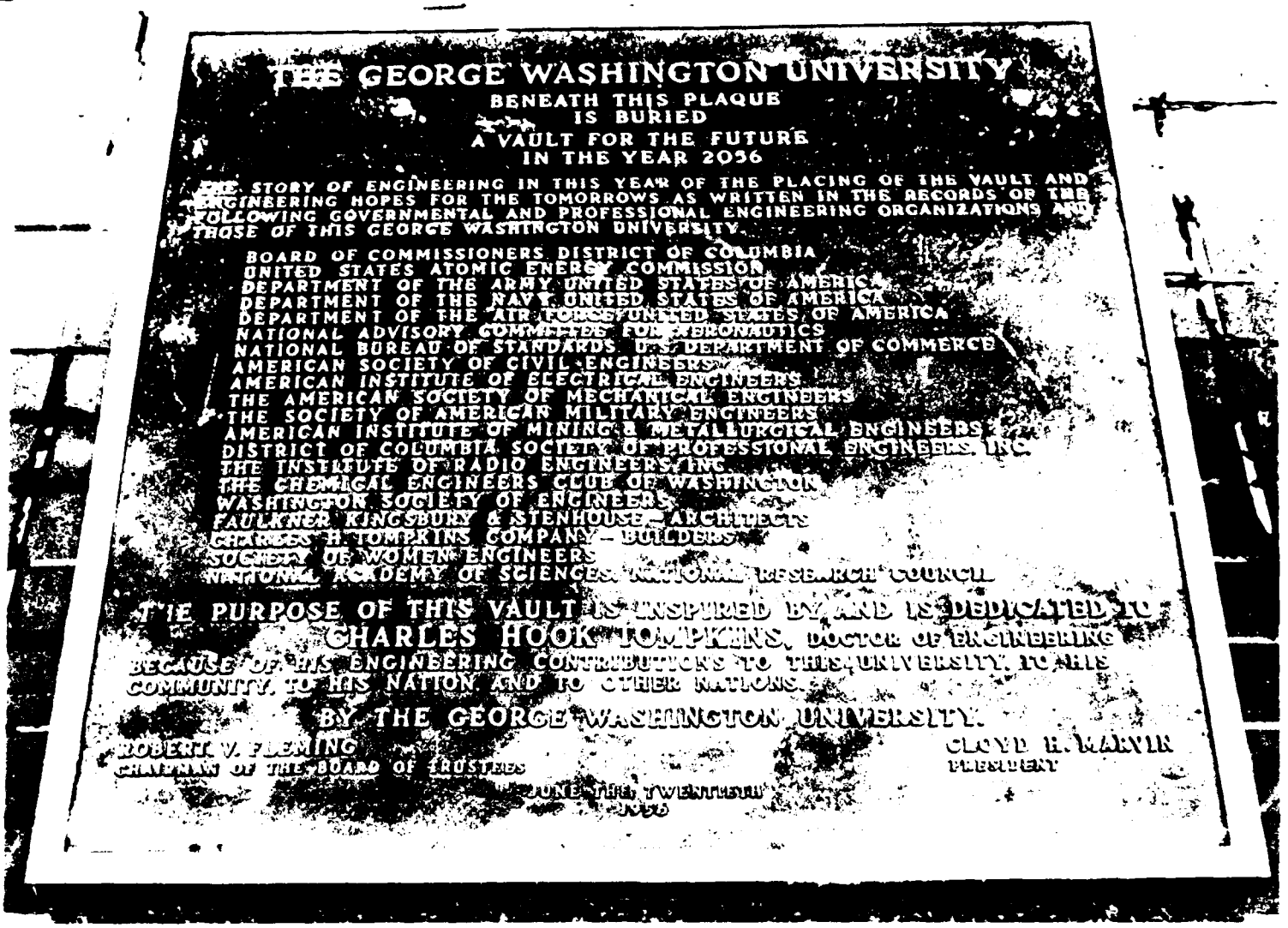

To cope with the expanding technology, our society must be assured of a continuing supply of rigorously trained and educated engineers. The School of Engineering and Applied Science is completely committed to this objective.